J|A|C|S COMMUNICATIONS

Published on Web 07/22/2010

# A Potential Site for Trapping Photogenerated Holes on Rutile $TiO_2$ Surface as Revealed by EPR Spectroscopy: An Avenue for Enhancing Photocatalytic Activity

Neeruganti O. Gopal,[†] Hsin-Hsi Lo,[†] Shiann-Cherng Sheu,[‡] and Shyue-Chu Ke*,[†]

*Physics Department and Nanotechnology Research Center, National Dong Hwa University, Hualien, Taiwan 97401, and Department of Occupational Safety and Health, Chang Jung Christian University, Tainan, Taiwan 711*

Received November 23, 2009; E-mail: ke@mail.ndhu.edu.tw

***Abstract:*** Rutile $TiO_2$ nanoparticles with new sites for effectively trapping photogenerated holes have been prepared by reacting the $TiO_2$ nanoparticles prepared in hydrogen atmosphere with molecular oxygen at elevated temperatures. The observed *g* values and the occurrence of $^{47}Ti$ and $^{49}Ti$ octet hyperfine pattern allowed us to assign this EPR active center to surface oxygen centered anion radical with two coordinating titaniums. The effective trapping of photogenerated holes by these new sites inhibits the electron−hole recombination and results in an enhanced photocatalytic activity under visible light by a factor of 2.5 compared with samples prepared parallel in air. Oxidation of reduced $TiO_2$ apparently is a simple low-cost and promising route for improving the photoactivity of $TiO_2$.

Titania ($TiO_2$) is the most commonly used photocatalyst in a number of technological fields.[1] The $TiO_2$ photocatalytic reaction is initiated by electron and hole generation upon band gap excitation. While a large portion of the photogenerated charge pairs recombine, a fraction of them diffuse to their respective surface traps. The surface-trapped electrons and trapped holes can also recombine or act as initiators for subsequent surface catalytic reactions. The photoefficiency of $TiO_2$ thus depends strongly on the trapping, recombination, and trap-state energetics. In this regard, electron paramagnetic resonance (EPR) spectroscopy has manifested itself in the identification of various trap sites for photogenerated electrons and holes. The electrons are trapped at coordinatively unsaturated cations located either on the surface or in the bulk of $TiO_2$ to form $Ti^{3+}$.[2] Two types of photogenerated holes have also being commonly observed:[2] holes trapped at the lattice oxygen atoms located in the subsurface layer with a structure of $[Ti^{4+}O^{-\bullet}Ti^{4+}OH^-]$ and holes trapped on the surface bridging oxygen atoms with a structure of $[Ti^{4+}O^{2-}Ti^{4+}O^{-\bullet}]$; they are designated as site A and B in Scheme 1, respectively. An understanding of the $TiO_2$ surface phenomena at the molecular level is of fundamental importance and is essential to improve or expand the scope of titania-based systems for specific applications.

It has been well established that, when a reduced $TiO_2$(110) crystal is exposed to $O_2$ at elevated temperatures, the Ti interstitials diffuse to the surface[3] and dissociate adsorbed $O_2$ molecule to form a surface $TiO_2$ island at the terrace,[3a] depicted as site C in Scheme 1. However, the role of site C in the photochemistry of titania has not been explored, and very little is known regarding the photoreactivity of reduced $TiO_2$ followed by oxidative treatment. The purpose of this study is to extend our knowledge of site C to evaluate its possible contribution to the photoactivity and to point the way toward future development of an efficient rutile $TiO_2$-based visible-light photocatalyst.

Following the protocol, oxidation of reduced rutile $TiO_2$ by $O_2$, reduced $TiO_2$ (*r*-$TiO_2$) nanoparticles were prepared by reacting $TiCl_4$ with benzyl alcohol at 80 °C along with continuous purging of the reaction vessel with 99.999% hydrogen gas. A parallel sample prepared in air (*air*-$TiO_2$) was used as a control for comparison (Figures S1−S4 and Table SI in Supporting Information). Reduced $TiO_2$ prepared by vacuum annealing results in the formation of bridging oxygen vacancies with two electrons which reduce the neighboring Ti atoms to form intrinsic EPR active $Ti^{3+}$, and that complicates the light-dependent EPR analysis. Also, although a bridging oxygen vacancy can serve as a channel for $O_2$ dissociation, it was found to be less efficient than the one associated with interstitial Ti.[3a] Thus, the vacuum-annealed sample was not subjected for further study. Both samples (*r*-$TiO_2$ and *air*-$TiO_2$) were then heated in air (exposure to $O_2$) at 800 °C. The $O_2$-exposed *r*-$TiO_2$ is termed *o-r*-$TiO_2$ hereafter. Both *o-r*-$TiO_2$ and *air*-$TiO_2$ do not exhibit any EPR signal in the dark (data not shown), i.e. they contain no bridging oxygen vacancy. Under visible light ($\lambda >$ 410 nm) irradiation, the EPR spectrum of *air*-$TiO_2$ (Figure 1a) exhibits signals at $g_1 = 2.0232$, $g_2 = 2.0162$, and $g_3 = 2.0049$ (signal I) and at $g_\perp = 1.9782$ and $g_\parallel = 1.9424$ (signal II) due to photogenerated holes and electrons, respectively, accumulated in the trapping sites of rutile.[2]

The EPR spectrum of *o-r*-$TiO_2$ (Figure 1b) under visible light contains the same signals as in *air*-$TiO_2$, but an additional set of trapped electron signals are observed at $g_\perp = 1.9707$ and $g_\parallel = 1.9504$ (signal

***Scheme 1.*** Model of Top Few Layers of Rutile $TiO_2$(110)[a]

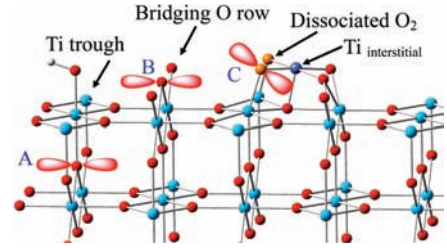


[a] Lattice Ti, cyanine; lattice O, red. Site A: trapped hole with OH group in the Ti trough. Site B: trapped hole at the surface bridging O. Site C: Ti interstitial (blue) diffused to the surface and dissociated adsorbed $O_2$ (O in orange) to form a $TiO_2$ cluster. Site C as a potential trap for photogenerated holes will be identified in this study. Only hole trap sites are shown for clarity.

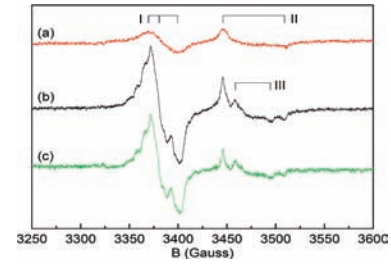


***Figure 1.*** EPR spectra measured at 5K for sample (a) *air*-$TiO_2$ and (b) *o-r*-$TiO_2$ under visible light illumination. (c) Difference spectrum between (b) and (a). Instrument settings: microwave frequency, 9.54004 GHz; microwave power, 3.16 mW; modulation amplitude, 2 G at 100 kHz.

[†] National Dong Hwa University.
[‡] Chang Jung Christian University.



**10.1021/ja909901f** 

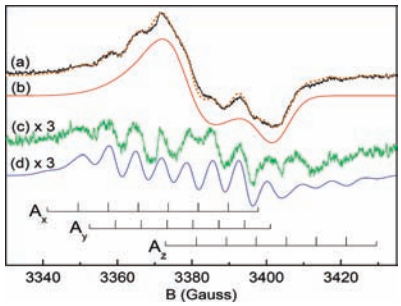


***Figure 2.*** Analysis of the hyperfine structure in the trapped hole region. (a) Duplicate of the hole signal portion of Figure 1c. (b) Simulation of (a) with only *g* splitting at 2.0228, 2.0185, and 2.0040. (c) Difference spectrum between (a) and (b) showing the unaccounted for multiline pattern. The spectrum is multiplied by a factor of 3 for clarity. (d) Simulation of (c) assuming an unpaired spin, with *g* values the same as those indicated above, interacting with either $I = 5/2$ (57.3%) nucleus or a $I = 7/2$ (42.7%) nucleus with hyperfine coupling constant $|A| = (22.8, 19.6, 22.8) \pm 0.5$ MHz that splits each principal *g* transition into a octet as indicated by the stick diagrams. The sum of the simulated spectra (b) and (d) is overlaid on the experimental spectra (a), shown in orange color.

III). Most likely, this new set of signals associates with Ti interstitial sites which act as trapping centers for photogenerated electrons, but with regard to its location, on the surface or in the subsurface layer, this cannot be specified. However, it is remarkably evident that in *o-r*-$TiO_2$ (Figure 1b), while the trapped electron signal shows only a moderate increase in its intensity, the double integrated intensity of hole signals has increased by a factor of ~4 when compared with that of *air-TiO*$_2$ (Figure 1a), indicating effective trapping of photogenerated holes in *o-r*-$TiO_2$.

A closer examination in the hole signal region of *o-r*-$TiO_2$ (Figure 1b) indicates that there are equally spaced hyperfine structure overlapped and superimposed on the broad signal, possibly with the most outer lines buried in the noise. Figure 2 presents analysis of the hyperfine pattern along with simulations. Species having nonzero nuclei spin with considerable natural abundance in $TiO_2$ are $^{47}$Ti ($I = 5/2$, 7.32%) and $^{49}$Ti ($I = 7/2$, 5.46%), which will give an eight-line hyperfine pattern with one line at each end having lower intensity than the others. We applied a hybrid genetic and simplex algorithm to search the six-dimensional parameter space of principal *g* and *A* values to find a unique solution of the spectrum. We found a very good fit, as depicted in Figure 2a (orange), with $g_{1,2,3} = (2.023, 2.019, 2.004)$ and $|A_{1,2,3}| = (22.8, 19.6, 22.8) \pm 0.5$ MHz. Stick diagrams (Figure 2, bottom) are constructed from the hyperfine coupling tensor denoting the calculated positions of the octet pattern for each principal *g*-direction, each of which is in good agreement with the observed hyperfine pattern. On the basis of point dipole−dipole approximation, we estimate that the distance between the unpaired spin and the magnetic Ti is 1.62 Å (Supporting Information).

A model for this new paramagnetic site can be developed on the basis of the following arguments. First, the unpaired electron is not centered on titanium (Supporting Information). Second, the derived *g* values strongly resemble those reported for the oxygen-centered anion radical ($O^{-\bullet}$) in the subsurface layer (site A, $g = 2.019, 2.014, 2.002$)[2] or on the surface (site B, $g = 2.026, 2.017, 2.008$)[2] produced by trapping photogenerated holes, suggesting a similar origin for this new trap site. However, no Ti hyperfine structure has ever been reported for hole traps in all phases of $TiO_2$, presumably because the Ti−O distance of ~1.95 Å for rutile and ~2.4 Å for anatase is long compared to 1.62 Å derived for the new trap site. Third, of particular importance, EPR distinction between holes trapped on the surface or in the subsurface layer is possible by considering the number of nearest titaniums surrounding the oxygen radical, two for surface hole and three for inner hole. Taking into account the isotopic abundance of Ti and the probability that the nearest-neighbor Ti sites of $O^{-\bullet}$ are occupied by one magnetic Ti, the calculated EPR intensity ratios due to nonmagnetic Ti and one magnetic Ti for one, two, and three nearest-neighbor Ti sites are 6.8, 3.4, and 2.3, respectively (Table S2, Supporting Information). The ratio of the double integrated intensity of the *g*-only spectrum (Figure 2b) and the magnetic Ti coupled spectrum (Figure 2c) is 3.37, which is in perfect agreement with the calculated values for two nearest-neighbor Ti nuclei. This strongly implies that the new paramagnetic site resides on the surface of $TiO_2$ and is coordinated by two titaniums. Finally, the Ti octet hyperfine pattern cannot be seen in the control sample prepared parallel in air (*air*-$TiO_2$) (Figure 1a). This implies that the new trap site must be associated with the reduced titania followed by interaction with $O_2$. These considerations led us to conclude that site C in Scheme 1 is responsible for trapping photogenerated valence band holes, giving rise to the observed EPR signal with Ti hyperfine structure.

We found that the reactivity of *o-r*-$TiO_2$ in visible light-activated methylene blue degradation exceeds that of *air*-$TiO_2$ by a factor of ~2.5 (Figure S6, Supporting Information). Because UV−vis, XPS, surface area, X-ray diffraction, and TEM of *o-r*-$TiO_2$ strongly resemble those of the control sample *air*-$TiO_2$ (Supporting Information) and the only difference between the two samples is the increases in the number of trapped electrons and trapped holes in *o-r*-$TiO_2$ upon light illumination (Figure 1) indicating effective charge carrier separation, we thus believe that the presence of site C in *o-r*-$TiO_2$ is solely responsible for the enhanced activity. As for how this site contributes to the enhanced photoreactivity, one explanation is that removal of free holes by hole trapping at site C, as evidenced by the 4-times increases in the trapped hole EPR signal, minimizes the electron−hole pair recombination because in the trapped state the hole is much less mobile toward a photogenerated electron than when it moves freely in the valence band. However, ultrafast time-resolved spectroscopy[4] following laser photolysis is required to elucidate the dynamics of charge carrier reaction within these particles.

In summary, a new surface center for effective trapping of photogenerated holes in rutile $TiO_2$ has been prepared by reacting $TiO_2$ prepared in $H_2$-atmosphere with $O_2$. Accordingly, the photoactivity of such samples exceeds that of samples prepared parallel in air by a factor of ~2.5. We believe efficient hole trapping is the origin for the enhanced photoactivity. We assign this new EPR active center to a surface oxygen centered anion radical with two coordinating titaniums at a shortened Ti−O distance, providing the first direct spectroscopic evidence for structural assignment of a trapped center in $TiO_2$. Since there is no need by external metal oxide coating or organic adlayers to the $TiO_2$ surface to provide spatial separation of the charge carriers, oxidation of reduced $TiO_2$ treatment is a simple and promising route for improving reactivity of $TiO_2$ by efficient hole trapping.

**Acknowledgment.** This work is supported by the National Science Council of Taiwan (NSC-98-2627-M-259-001).

**Supporting Information Available:** material characterization, EPR analysis, and activity data. This material is available free of charge via the Internet at http://pubs.acs.org.

## References

(1) (a) Linsebigler, A. L.; Lu, G.; Yates, J. T., Jr. *Chem. Rev.* **1995**, *95*, 735. (b) Thompson, T. L.; Yates, J. T., Jr. *Chem. Rev.* **2006**, *106*, 4428. (c) Chen, X; Mao, S. S. *Chem. Rev.* **2007**, *107*, 2891.
(2) Kumar, C. P.; Gopal, N. O.; Wang, T. C.; Wong, M. S.; Ke, S. C. *J. Phys. Chem. B* **2006**, *110*, 5223. and references therein.
(3) (a) Wendt, S.; Sprunger, P. T.; Lira, E.; Madsen, G. K. H.; Li, Z.; Hansen, J. O.; Matthiesen, J.; Blekinge-Rasmussen, A.; Laegsgaard, E.; Hammer, B.; Besenbacher, F. *Science* **2008**, *320*, 1755. (b) Iddir, H.; Ogut, S.; Zapol, P.; Browning, N. D. *Phys. Rev. B* **2007**, *75*, 073203. (c) Bennett, R. A.; Stone, P.; Price, N. J.; Bowker, M. *Phys. Rev. Lett.* **1999**, *82*, 3831. (d) Li, M.; Hebenstreit, W.; Gross, L.; Diebold, U.; Henderson, M. A.; Jennison, D. R.; Schultz, P. A.; Sears, M. P. *Surf. Sci.* **1999**, *437*, 173. (e) Valden, M.; Lai, X.; Goodman, D. W. *Science* **1998**, *281*, 1647.
(4) (a) Rothenberger, G.; Moser, J.; Gratzel, M.; Serpone, N.; Sharma, D. K. *J. Am. Chem. Soc.* **1985**, *107*, 8054. (b) Leytner, S.; Hupp, J. T. *Chem. Phys. Lett.* **2000**, *330*, 231. (c) Yamakata, A.; Ishibashi, T.; Onishi, H. *Chem. Phys. Lett.* **2001**, *333*, 271.

JA909901F